Strong phonon charge carrier coupling in thermoelectric clathrates

Anders Bentien, Simon Johnsen, and Bo Brummersted Iversen*
Department of Chemistry, University of Aarhus, Langelandsgade 140, 8000 Aarhus C, Denmark
(Received 13 October 2005; revised manuscript received 23 January 2006; published 2 March 2006)

The origin of the very low and glasslike lattice thermal conductivity (κ_L) in highly crystalline clathrates has been intensely discussed. Guest atom tunneling, guest atom resonant scattering, disorder scattering, and soft potentials have been proposed as possible explanations. However, none of these models can explain the fundamental difference in κ_L between *n*- and *p*-type $Ba_8Ga_{16}Ge_{30}$. Here we provide a comprehensive explanation through analysis of the physical properties of a range of $Ba_8In_{16-x}Ge_{30-y}\square_{x+y}$ and $Ba_8Ni_{6-x}Ge_{40+x}$ samples. We show that κ_L is intimately linked to the charge carriers, and propose that the glasslike κ_L is a consequence of strong phonon charge carrier coupling. In general the influence of charge carriers on κ_L has been studied only in relatively lightly doped and structurally ordered semiconducting materials. Clathrates constitute a class of materials with relatively large charge carrier concentrations in combination with structural disorder. This opens up the possibility of studying the influence of charge carriers on κ_L in the limit where κ_L and κ_e are of equal magnitude.

DOI: 10.1103/PhysRevB.73.094301 PACS number(s): 63.20.−e, 72.15.−v, 72.20.−i

Inorganic clathrates are Zintl compounds with alkali or alkaline earth elements located inside cages made from tetrahedrally bonded group IV atoms partly substituted by group III or transition elements to ensure charge compensation. The lattice thermal conductivity (κ_L) of clathrates has been intriguing since the discovery of the glasslike magnitude and temperature dependence of κ_L in *n*-type $Sr_8Ga_{16}Ge_{30}$ (Ref. 1) and *n*-type $Eu_8Ga_{16}Ge_{30}$.[2] Initially it was proposed that guest atom tunneling in combination guest atom resonant phonon scattering was responsible for the glasslike κ_L.[2–5] This appeared to be corroborated by the absence of a glasslike κ_L in *n*-type $Ba_8Ga_{16}Ge_{30}$, where neutron diffraction experiments showed that the cation nuclear density distribution is more localized than in $Sr_8Ga_{16}Ge_{30}$ and $Eu_8Ga_{16}Ge_{30}$.[4] However, later a glasslike κ_L was also observed in *p*-type $Ba_8Ga_{16}Ge_{30}$, and it was proposed that the low temperature ($T<5-10$ K) κ_L is determined by phonon charge carrier scattering.[6] The dip in κ_L observed at approximately 10–30 K, which is believed to originate from phonon resonant scattering on guest atoms, was suggested to be enhanced by some unknown mechanism related to the electronic band structure.[6] Disorder scattering related to the displacement of the guest atoms,[7] four well tunneling,[8] as well as soft potential model for the guest atoms[9] have been proposed as models for explaining the dip in κ_L. However, all the models lack the ability to explain the difference in κ_L between the almost identical crystal structures of *n*- and *p*-type $Ba_8Ga_{16}Ge_{30}$.[10]

Here we present $\kappa_L(T)$ data of four $Ba_8In_{16-x}Ge_{30-y}\square_{x+y}$ samples ($\square$ is a vacancy) and four $Ba_8Ni_{6-x}Ge_{40+x}$ samples along with some of their electronic properties. $\kappa_L(T)$ varies from normal crystal-like to glasslike, and together with the systematic changes in the electronic properties this is convincing empirical evidence that the scattering mechanisms determining $\kappa_L(T)$ of clathrates are linked to the charge carriers. We propose that the glasslike thermal conductivity is a consequence of two different phonon charge carrier scattering mechanisms. The first mechanism is due to phonons scattered from free charge carriers and this mechanism dominates at $T<5-10$ K leading to $\kappa_L(T)\propto T^2$.[6,10] The second mechanism, which is responsible for the resonance dip in $\kappa_L(T)$ at approximately 10–30 K, is related to phonons scattered from bound/localized charge carrier states. As a consequence of this we believe that the resonant scattering of phonons on the guest atoms only contributes significantly to the thermal resistance above 50–70 K. This is in accordance with recent values of resonance frequencies of the guest atoms[11] which are found to be too high to be related to the resonance dip.

Table I lists the samples used in the present study along with various chemical and physical properties. The earliest records on $Ba_8In_{16-x}Ge_{30-y}\square_{x+y}$ and $Ba_8Ni_6Ge_{40}$ are in Refs. 12 and 13, respectively. Samples Ia and Ib were synthesized by heating Ba, In, and Ge (8:16:30) in an evacuated quartz ampoule up to 1000 °C followed by a rapid cooling to room temperature. The products were crushed into fine powders and hot pressed. Sample Ia was pressed with a 30 MPa pressure at 575 °C for 15 min, but this resulted in elemental indium being pressed out of the sample. From the mass of the In the empirical formula of the bulk material could be estimated to $Ba_8In_{12.9}Ge_{30}$. Sample Ib was pressed at only 500 °C (also 30 MPa), but this still leads to In being pressed out of the sample. For this sample the empirical formula was estimated to be $Ba_8In_{12.2-13.3}Ge_{30}$. After pressing both samples were annealed at 600 °C for 4 days. Samples Ic and Id were synthesized by an In-flux method similar to the one described in Ref. 6. Excess amounts of In with Ba and Ge in a 8:30 relationship were heated to 1000 °C in an evacuated quartz ampoule, and subsequently cooled at 2 °C/h to 600 °C (sample Ic) and room temperature (sample Id). Large single crystals (diameters >5 mm) were found after removing the excess indium by heating followed by soaking the products in concentrated HCl for several hours. $Ba_8Ni_{6-x}Ge_{40+x}$ samples with $x=0$ (IIa), 0.2 (IIb), 0.4 (IIc), and 0.6 (IId) were synthesized by heating stoichiometric amounts of the elements in evacuated carbon coated quartz

TABLE I. Measured and calculated chemical and physical properties. The composition of the indium containing clathrates was estimated by energy dispersive x-ray analysis (EDX) and the results are given relative to sample Id which was assumed to have $Ba_8In_{16}Ge_{30}$ composition. This assumption seems to be justified since the lattice parameter of sample Id is close to the lattice parameter of the $Ba_8In_{16}Ge_{30}$ sample in Ref. 12. The relative uncertainty in the composition measurement is of the order 1% leading to an uncertainty of 0.1–0.3 in the composition of the samples. The composition of the Ni containing clathrates is taken as the nominal composition. The third column refers to the crystallinity, pc and sc is poly and single crystalline, respectively. n and p refers to n- or p-type. The lattice parameters were determined from conventional powder diffraction data with LaB_6 (a=4.15692 Å at 23 °C) as internal standard. Densities were measured using Archimedes' principle on a home-built device. The charge carrier density (n in units of e per unit cell) is calculated from the Hall resistivity measured as function of magnetic field (0–9 T). ρ is the resistivity and S is the thermopower. The effective mass (m^*) is calculated from n and the thermopower. l is the mean free path of the charge carriers, μ is the Hall mobility, and $\rho_{400\ K}/\rho_{2\ K}$ is the residual resistance ratio. The m or s in parenthesis refers to whether the temperature dependence of ρ is metal- or semiconductor-like. For all properties the subscript refers to the temperature of the measurement.

	Composition	Crystallinity	$a_{295\ K}$ (Å)	ρ_{meas} (g/cm^3)	ρ_{meas}/ρ_{theo} (%)	$n_{300\ K}$ (e/uc)	$\rho_{300\ K}$ ($\mu\Omega$ cm)	$S_{400\ K}$ (μV/K)	m^*/m_0	$l_{300\ K}$ (Å)	$\mu_{300\ K}$ (cm^2 s^{-1} V^{-1})	$\rho_{400\ K}/\rho_{2\ K}$
Ia	$Ba_8In_{13.3(2)}Ge_{28.6(3)}\square_{4.1}$	pc/n	11.1785(6)	5.57	100	−3.7	1339	−75	5.4	5.0	1.8	1.6 (m)
Ib	$Ba_8In_{12.8(2)}Ge_{29.8(3)}\square_{3.4}$	pc/n	11.1819(18)	5.45	97	−5.2	1126	−73	6.6	4.7	1.5	2.0 (m)
Ic	$Ba_8In_{16.1(2)}Ge_{29.9(3)}$	sc/n	11.2153(4)	6.02	100	−6.5	574	−52	5.4	8.0	2.3	8 (m)
Id	$Ba_8In_{16}Ge_{30}$	sc/n	11.2202(9)	6.02	100	−4.3	1211	−87	6.7	5.0	1.7	2.2 (m)
IIa	$Ba_8Ni_6Ge_{40}$	pc/p	10.6764(3)	5.97	100	9.6	2512	126	17	1.5	0.41	0.89 (s)
IIb	$Ba_8Ni_{5.8}Ge_{40.2}$	pc/p	10.6776(3)	5.75	97	5.4	3889	146	15	1.4	0.42	0.54 (s)
IIc	$Ba_8Ni_{5.6}Ge_{40.4}$	pc/n	10.6795(2)	5.72	96	−0.32	7965	−104	2.2	3.9	2.9	0.26 (s)
IId	$Ba_8Ni_{5.4}Ge_{40.6}$	pc/n	10.6807(4)	5.83	98	−0.52	3663	−144	3.0	7.0	4.8	1.1 (s)

ampoules up to 1000 °C for 2 h followed by slow cooling to 700 °C. The samples were held at this temperature for 48 h and subsequently quenched to room temperature. The products were crushed into fine powders from which pressed samples were made by a spark plasma sintering. Sample IIa was heated to 575 °C with a 75 MPa pressure, whereas the other three samples only were heated to 500 °C. On all samples the purity was checked by conventional powder x-ray diffraction on a Bruker D8 diffractometer (Cu Kα). Small amounts (1 to 2 at. %) of elemental indium were found in samples Ia and Ib. For samples Ic and Id no other phases were observed. However, the resistivity measurement showed a superconducting transition around 3.5 K and this is probably a small amount of excess In not removed by the acid treatment. In samples IIa–IId small impurities of NiGe were detected by conventional x-ray powder diffraction. Sample IIb was also used in a synchrotron powder diffraction study and here the amount of NiGe could be refined to 1.52 w/w %.[14] A trace of $BaGe_2$ was also detected, but the refinements did not converge if this phase was included (peak intensities were very small). The thermal conductivity (κ), thermopower (S), resistivity (ρ), and Hall effect (R_H) were measured on a Quantum Design Physical Properties Measurement System. The lattice thermal conductivities of the samples are plotted in Fig. 1.

Among the indium containing clathrates the lattice parameter (a) varies significantly between the hot pressed samples and the samples grown in indium flux, Table I. This variation can be explained by the difference in the composition and the relatively large concentration of vacancies in samples Ia and Ib. The small difference in a between samples Ic and Id can be explained by a slightly larger In content in sample Id due to different synthesis conditions. The compositions, densities, and lattice parameters of Ia and Ib are at variance with the $Ba_8In_xGe_{42-3/4x}\square_{4-1/4x}$ composition suggested in Ref. 12, and this indicates a significant In, Ge, and □ phase width. For the nickel containing clathrates a increases slightly with increasing Ge content. In general, one vacancy in a tetrahedral coordination environment leads to eight localized states, i.e., two states from each dangling bond next to the vacancy. Energetically these states are located in the band gap, and if the vacancy concentration is sufficiently large a band can be formed.[15,16] Thus compared with a framework without a vacancy eight states are removed from the valence band. From the composition of samples Ia and Ib the total number of valence electrons per unit cell is 170.2 and 173.6 e^-/uc, respectively. The total number of valence states and localized states due to vacancies are 151.1 per uc (156.9 per uc for Ib) and 32.9 per uc (27.1 per uc for Ib), respectively. This means that the Fermi levels in these two samples are located in localized vacancy bands, and this explains the n-type electrical properties with relatively large carrier concentration (n), large effective mass (m^*), and low mobility (μ), see Table I. For samples Ic and Id n-type properties are also observed, although with a charge carrier concentration much larger than expected if the composition is close to the ideal 8:16:30 ratio. Nonetheless it can be explained by the presence of vacancies with a concentration that does not exceed one per unit cell. This is smaller than can be detected by diffraction but still in agreement with the measured/theoretical densities, large m^* and low μ. For $Ba_8Ni_{6-x}Ge_{40+x}$, the IIa (x=0) and IIb (x=0.2) samples show p-type properties, whereas the other two samples (IIc, IId) have n-type properties. From valence electron counting one would expect p-type properties for all samples with n=8, 7.2, 6.4, and 5.6 e^+/uc for samples IIa–IId, respectively. Only samples IIa and IIb have

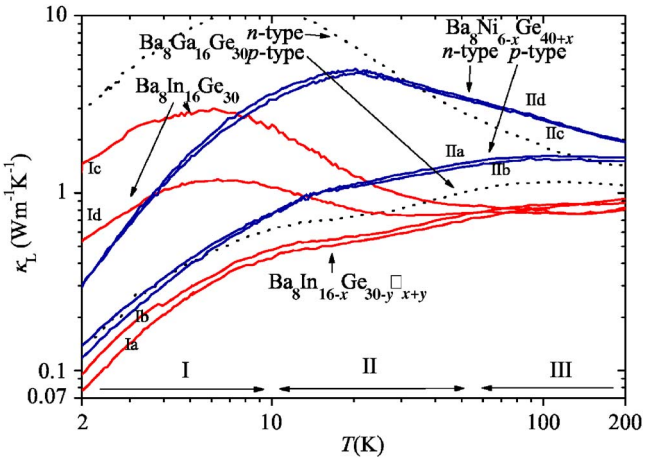

FIG. 1. (Color online) Lattice thermal conductivity (κ_L) as function of temperature (T) for the $Ba_8In_{16-x}Ge_{30-y}\square_{x+y}$ [red (light) curves] and $Ba_8Ni_{6-x}Ge_{40+x}$ [blue (dark) curves]. Included is also κ_L of one p-type and one n-type $Ba_8Ga_{16}Ge_{30}$ (black dotted curves) from Ref. 6. κ_L has been calculated from $\kappa=\kappa_L+\kappa_c$, where κ is the measured thermal conductivity and κ_c is the charge carrier contribution calculated from resistivity using the Wiedemann-Franz law and assuming that the carriers are degenerate. At 200 K κ_c varies among all samples from 0.05 W m^{-1} K^{-1} (IIc) to 1.1 W m^{-1} K^{-1} (Ic). At 10 K the corresponding values are 0.001 W m^{-1} K^{-1} (IIc) to 0.26 W m^{-1} K^{-1} (Ic). The romans letters at the bottom refer to ranges where phonon charge carrier scattering dominates (I), phonon scattering on localized electronic states dominates (II), and resonant scattering of the phonons on the guest atoms dominates (III).

charge carrier concentrations close to the expected, Table I. Since only small amounts of impurity phases are observed and a increases systematically with Ge content, deviations from the nominal stoichiometry seems an unlikely explanation for the n-type properties, which are probably due to the presence of a small amount of vacancies. One striking feature is the very large m^* ($\sim 15\ m_0$) and very low μ and mean free path (l) of the charge carriers in the p-type $Ba_8Ni_{6-x}Ge_{40+x}$ samples.

In Fig. 1 the lattice thermal conductivities of the eight samples are plotted. For $Ba_8In_{16-x}Ge_{30-y}\square_{x+y}$ the two samples with a large concentration of vacancies (Ia and Ib) have κ_L temperature dependencies similar to the glasslike thermal conductivity observed for n-type $Sr_8Ga_{16}Ge_{30}$,[1] n-type $Eu_8Ga_{16}Ge_{30}$,[2,5,10] and p-type $Ba_8Ga_{16}Ge_{30}$.[6] Samples Ic and Id have more crystal-like κ_L, although the thermal conductivity of sample Id reaches a value of only ~ 1 W m^{-1} K^{-1} at 8 K. For $Ba_8Ni_{6-x}Ge_{40+x}$ the thermal conductivities of the two n-type samples are very similar and crystal-like, whereas for the two p-type samples the magnitude of κ_L is much reduced with glasslike temperature dependencies, although the dip observed around 10–30 K in other glasslike clathrates is less pronounced.

In a recent paper[11] we pointed out that higher values of the guest atom resonance frequencies are obtained from diffraction experiments and specific heat data on one side than from inelastic neutron scattering, Raman spectroscopy, and acoustic attenuation on the other. Based on the differences in $\kappa_L(T)$ of p- and n-type $Ba_8Ga_{16}Ge_{30}$ we have earlier proposed that the low temperature ($T<5-10$ K) κ_L is determined by phonon charge carrier scattering.[6] Here we extend the argumentation and propose that the resonance dip in $\kappa_L(T)$ is also due to phonon charge carrier scattering, and that resonant scattering from the guest atoms only plays a role above $\sim 50-70$ K in agreement with the resonance frequencies obtained from scattering experiments and specific heat data. It has been shown earlier that phonon charge carrier scattering has a significant contribution to the thermal resistivity below ~ 10 K.[6,10] We believe the most appropriate model for describing $\kappa_L(T)$ below 5–10 K is the free electron model by Ziman.[17,18] This type of scattering gives a T^2 temperature dependence of κ_L and a scattering rate which increases with m^{*2}. Later extensions of the theory have shown that in disordered materials the scattering rate can increase further if $ql<1$, where q is phonon wave number.[19]. Furthermore, the condition that only phonons with $q<2k_F$ can be scattered may be relaxed, and this extension can lead to scattering at even higher temperatures.[20] Another type of scattering mechanism, which has not been considered as contributing to the κ_L resonance dip, is phonon scattering on degenerate electronic impurity/localized states. These states can be dynamically Jahn-Teller split by a local phonon distortion of the lattice.[21–23] This scattering mechanism is difficult to quantify, but as seen from Figs. 3 and 4 in Ref. 21 sufficiently high impurity concentrations ($\sim 10^{26}-10^{27}$ m^{-3}) in Si and GaAs result in κ_L having a resonance dip and magnitude similar to what is observed in clathrates. In the clathrates the impurity/localized states originate from either vacancies or the disorder among the framework atoms. Qualitatively $\kappa_L(T)$ therefore can be explained in terms of the two phonon charge carrier scattering mechanisms at low temperature and guest atom resonance scattering at higher temperatures. The glasslike κ_L of samples Ia and Ib, and crystal-like κ_L of samples Ic and Id can be interpreted as a consequence of larger vacancy concentrations in the former which introduces the localized/impurity states that can lead to resonancelike scattering. At higher temperatures $\kappa_L(T)$ converges towards the same value for all $Ba_8In_{16-x}Ge_{30-y}\square_{x+y}$ samples as expected if guest atom resonant scattering dominates. It is interesting to note that the more metal-like samples (larger n, smaller ρ, and larger residual resistance ratio) Ic and to a lesser extent Ib, have a larger κ_L than samples Id and Ia, respectively, below approximately 50 K. Such a systematic dependence on the electrical properties is also observed for $Sr_8Ga_{16}Ge_{30}$,[1,10] $Eu_8Ga_{16}Ge_{30}$,[10] and $Ba_8Ga_{16}Ge_{30}$ (Ref. 6) and can partly be explained by a lower l of samples with lower n.[6,10]

For $Ba_8Ni_{6-x}Ge_{40+x}$ the framework structure is more ordered with the Ni atoms preferring to occupy the 6c site.[13]. In this case the number of impurity/localized states is reduced, and consequently the resonance scattering is reduced giving no clear dips in $\kappa_L(T)$ of any of the $Ba_8Ni_{6-x}Ge_{40+x}$ samples. The difference in $\kappa_L(T)$ between n- and p-type $Ba_8Ni_{6-x}Ge_{40+x}$ can be explained by the large m^* in p-type $Ba_8Ni_{6-x}Ge_{40+x}$ which enhances the phonon scattering on free charge carriers. Between the two n- or the two p-type samples the variation of $\kappa_L(T)$ is within the resolution of the

measurement. From our model one could expect variations because of differences in n, l, and m^*. However, the main point is the very large difference between n- and p-type samples.

For $Ba_8Ga_{16}Ge_{30}$ measurements of the transport properties indicate that the number of localized states close to the valence band is much larger than the number of localized states close to the conduction band. All p-type $Ba_8Ga_{16}Ge_{30}$ samples in the literature have thermally activated transport properties, even when the charge carrier concentration is as high as 0.6 e^+/uc.[6,24] For n-type $Ba_8Ga_{16}Ge_{30}$ samples thermally activated behavior has not been observed even though samples with a charge carrier concentration as low as 0.2 e^-/uc[24] have been measured. A qualitative reason is that a Ga impurity in an ordered $Ba_8Ga_{16}Ge_{30}$ lattice acts as an acceptor, with localized acceptor states close to the valence band only. This result is in good qualitative agreement with the proposed phonon charge carrier scattering model and that glasslike $\kappa_L(T)$ is only observed in p-type $Ba_8Ga_{16}Ge_{30}$. For $Sr_8Ga_{16}Ge_{30}$ and $Eu_8Ga_{16}Ge_{30}$ samples a glasslike $\kappa_L(T)$ is also observed in metallic samples. Nonetheless, two $Sr_8Ga_{16}Ge_{30}$ samples that exhibit metallic properties with a very low ρ and a large RRR have a normal crystal-like $\kappa_L(T)$,[25] and the general trend among $Sr_8Ga_{16}Ge_{30}$ and $Eu_8Ga_{16}Ge_{30}$ samples is that as n decreases the more glasslike $\kappa_L(T)$ becomes.[10] This is an indication that Ga/Ge disorder (localized) states play a role and that the Ga/Ge disorder in $Sr_8Ga_{16}Ge_{30}$ and $Eu_8Ga_{16}Ge_{30}$ is larger than in $Ba_8Ga_{16}Ge_{30}$.

We have presented $\kappa_L(T)$ data for eight samples, which together with literature data give convincing empirical evidence that the glasslike κ_L is linked to the electronic properties. The glasslike κ_L (and absence thereof) can be qualitatively explained by phonon scattering on free charge carriers in combination with scattering on bound charge carriers, the latter being responsible for the resonance dip in κ_L. Thus the results from Raman spectroscopy[26] and ultrasonic experiments[8,27] should be interpreted in terms of phonon charge carrier scattering/coupling. The reduction of the elastic constants observed at low temperatures,[8] which for clathrates has been interpreted as being due to tunneling states, is in fact also seen in p-type silicon.[28] In Si the reduction is related to the localized states of the dopant atoms.

We would like to thank the Carlsberg Foundation and the Danish Research Councils for funding a PPMS. The Danish Technical Research Council (A.B.) and the Danish Strategic Research Council (S.J.) are thanked for partly funding the work. M. Christensen is thanked for valuable discussions.

*Corresponding author. Email address: bo@chem.au.dk

[1] G. S. Nolas, J. L. Cohn, G. A. Slack, and S. B. Schujman, Appl. Phys. Lett. **73**, 178 (1998).
[2] J. L. Cohn, G. S. Nolas, V. Fessatidis, T. H. Metcalf, and G. A. Slack, Phys. Rev. Lett. **82**, 779 (1999).
[3] G. S. Nolas, T. J. R. Weakley, J. L. Cohn, and R. Sharma, Phys. Rev. B **61**, 3845 (2000).
[4] B. C. Sales, B. C. Chakoumakos, R. Jin, J. R. Thompson, and D. Mandrus, Phys. Rev. B **63**, 245113 (2001).
[5] S. Paschen, W. Carrillo-Cabrera, A. Bentien, V. H. Tran, M. Baenitz, Y. Grin, and F. Steglich, Phys. Rev. B **64**, 214404 (2001).
[6] A. Bentien, M. Christensen, J. D. Bryan, A. Sanchez, S. Paschen, F. Steglich, G. D. Stucky, and B. B. Iversen, Phys. Rev. B **69**, 045107 (2004).
[7] F. Bridges and L. Downward, Phys. Rev. B **70**, 140201(R) (2004).
[8] I. Zerec, V. Keppens, M. A. McGuire, D. Mandrus, B. C. Sales, and P. Thalmeier, Phys. Rev. Lett. **92**, 185502 (2004).
[9] K. Umeo, M. A. Avila, T. Sakata, K. Suekuni, and T. Takabatake, J. Phys. Soc. Jpn. **74**, 2145 (2005).
[10] A. Bentien, V. Pacheco, S. Paschen, Y. Grin, and F. Steglich, Phys. Rev. B **71**, 165206 (2005).
[11] A. Bentien, E. Nishibori, S. Paschen, and B. B. Iversen, Phys. Rev. B **71**, 144107 (2005).
[12] B. Kuhl, A. Czybulka, and H. U. Schuster, Z. Anorg. Allg. Chem. **621**, 1 (1995).
[13] G. Cordier and P. Woll, J. Less-Common Met. **169**, 291 (1991).
[14] S. Johnsen, A. Bentien, B. Iversen, and M. Nygren (unpublished).
[15] N. F. Mott, *Conduction in Non-Crystalline Materials* (Clarendon Press, Oxford, 1993).
[16] H. Y. Fan, Solid State Phys. **1**, 283 (1955).
[17] J. M. Ziman, Philos. Mag. **1**, 191 (1956); **2**, 292(E) (1956).
[18] J. M. Ziman, *Electrons and Phonons* (Oxford University Press, New York, 1960).
[19] A. Sergeev and V. Mitin, Europhys. Lett. **51**, 641 (2000).
[20] M. Singh and G. S. Verma, J. Phys. C **7**, 3743 (1974).
[21] J. Maier and E. Sigmund, J. Phys. C **17**, 4141 (1984).
[22] A. Puhl, E. Sigmund, and J. Maier, Phys. Rev. B **32**, 8234 (1985).
[23] J. Maier and E. Sigmund, Phys. Rev. B **34**, 5562 (1986).
[24] H. Anno, M. Hokazono, M. Kawamura, J. Nagao, and K. Matsubara, in *Proceedings of the 21st International Conference on Thermoelectrics* (IEEE, New York, 2002), p. 77.
[25] C. Uher, J. H. Yang, and S. Q. Hu, Mater. Res. Soc. Symp. Proc. **545**, 247 (1999).
[26] G. S. Nolas and C. A. Kendziora, Phys. Rev. B **62**, 7157 (2000).
[27] V. Keppens, M. A. McGuire, A. Teklu, C. Laermans, B. C. Sales, D. Mandrus, and B. C. Chakoumakos, Physica B **316**, 95 (2002).
[28] W. P. Mason and T. B. Bateman, Phys. Rev. **134**, A1387 (1964).